ISBN: 978-3-95450-191-5 doi:10.18429/JACoW-SRF2017-TUPB070

INFN-LASA CAVITY DESIGN FOR PIP-II LB650 CAVITY

C. Pagani[1], J.F. Chen†, M. Bertucci, A. Bignami, A. Bosotti, P. Michelato
L. Monaco, R. Paparella, D. Sertore, INFN-LASA, Segrate (MI), Italy
S. Pirani, ESS, Lund, Sweden
[1]also at University of Milan, Milan, Italy

Abstract

INFN-LASA is going to join the international partnership for Fermilab PIP-II project and to provide a novel design for the 650 MHz cavity of the 0.61 beta linac section, plug compatible with the Fermilab Cryomodule design. This paper reports the cavity design features both from the ElectroMagnetic and mechanical aspects, with focus on the rationales at the basis of the choice of main parameters. Furthermore, the current plans for the future R&D activity are here reported, including the ongoing production of three single cells and two complete cavities with our LB650 prototype design.

INTRODUCTION

The Fermilab PIP-II Linac is designed to deliver an average proton beam current of 2 mA at an energy of 800 MeV, to be fully compatible with Continuous Wave (CW) operation [1]. One main section of the Linac is the 650 MHz superconducting part of β_G = 0.61 that contains 33 five-cell cavities, accelerating proton beam from 185 MeV to 500 MeV.

INFN-LASA is going to join the international partnership to provide a novel design for the LB650 cavities, fully plug compatible with the Fermilab Cryomodule design, i.e. beam pipes, couplers, Helium tank, tuners and so on.

This paper describes the INFN-LASA design of LB650 cavity, including both ElectroMagnetic (EM) and mechanical designs with detailed reasons for the choice of geometric parameters. Based on this choices, three single-cell prototypes are being fabricated to validate the design, and to explore the road for the development of five-cell cavities in near future, being two complete cavities already planned.

CAVITY DESIGN

PIP-II cavities are required to be compatible with CW operation. Since in this CW operational mode, the RF duty factor is not a knob for tuning the dynamic heat load, a high accelerating efficiency in terms of R/Q is instead necessary. A high R/Q of cavity principally requires small iris aperture and small wall-angle; this may lead to difficulties in Field Flatness tuning, cavity surface treatment and cleaning. In addition, the relatively small beam current of PIP-II results in high external Q (Q_{ex}) of the cavity that implies a narrow bandwidth of the accelerating mode. In order to have a stable beam acceleration, a strict control of the Lorentz Force Detuning and microphonic is required, not only with stiffening rings but also by a proper shape of the cells. Our cavity design considers all these effects and aims to have an optimal balance between the multiple geometric parameters.

Our goal in designing the cavity is to achieve as high as possible accelerating efficiency with acceptable cell-to-cell coupling, and as low as possible pressure sensitivity and Lorentz Force Detuning (LFD) coefficient with modest cavity stiffness, to allow cavity tuning.

Firstly, we will describe the process to reach the minimum acceptable cell-to-cell coupling while maximizing the R/Q. Secondly, we explain the relationship between LFD and geometric parameters. At last, we adjust the radius of the stiffening ring to achieve a relatively low-pressure sensitivity.

Rationales

The cavity parameter R/Q is mainly determined by aperture sizes. A smaller aperture is preferred for high R/Q, even if this choice decreases significantly the cell-to-cell coupling, k_{cc}. The k_{cc} obviously affects the sensitivity of the field profile of the π-mode to frequency error of individual cells. This field flatness sensitivity is measured by the ratio [2, 3]:

$$N^2/(\beta k_{cc})$$

where N is the number of cells, β is the relative velocity and k_{cc} is the cell-to-cell coupling.

It is favourable to keep this ratio low. A list of some successful cavities is used for comparison, as shown in Table 1. Taking TESLA ratio as reference, the PIP-II LB650 cavity shall have $k_{cc} \geq 0.95\%$.

Table 1: Comparison of Cell-to-Cell Coupling

Cav	N	β	k_{cc} (%)	$N^2/(\beta k_{cc})$
TESLA	9	1	1.87	4331
SNS MB	6	0.61	1.52	3883
ESS MB	6	0.67	1.55	3467
PIP-II LB650	5	0.61	**0.95**	4331

The Buildcavity [4] and Superfish [5] codes are used for the cavity design. In Buildcavity, seven parameters are used to determinate a half-cell: R_{iris}, D, alpha, R, r, d and L, corresponding to iris radius, equator diameter, side wall angle, equator elliptical ratio (B/A), iris elliptical ratio (b/a) and length, as shown in Figure 1.

The half-cell shape is designed iteratively. Starting from an initial half-cell shape with Riris =48.0 mm, D=196.0 mm , alpha= 2°, R=1, r=1.7, d= 14 mm and L =70.4 mm, we change only the iris radius to find the relationship between k_{cc} and R/Q. Figure 2 shows both the k_{cc} and R/Q versus R_{iris}. As we can see, the cell-to-cell coupling monotonically decreases with the rising R/Q. Due to this reason, the k_{cc} = 0.95% is chosen to obtain the maximum R/Q. Meanwhile, the iris diameter of 88 mm can be fixed.

† email address: jinfang.chen@mi.infn.it

ISBN: 978-3-95450-191-5 doi:10.18429/JACoW-SRF2017-TUPB070

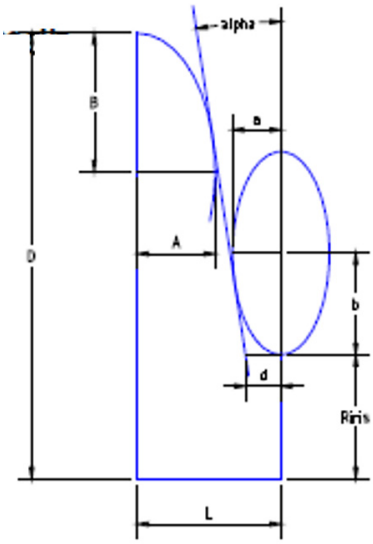

Figure 1: Seven parameters used to define a half-cell.

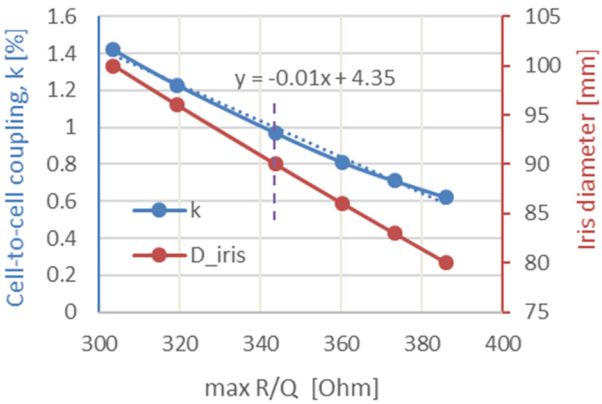

Figure 2: The relationship of cell-to-cell coupling and iris diameter vs R/Q.

We have studied also the relationship between LFD and R_{iris} with a fixed stiffening-ring radius at 70 mm. In order to have a clear trend of LFD versus R_{iris}, among the seven HC parameters, only R_{iris} is changed, other parameters kept constant except D that has been changed to tune the HC at the correct frequency. As shown in Figure 3, the trend shows that a smaller iris aperture is favoured for LFD. Notes that the LFD dependence is much sharper when R_{iris} is above 50 mm.

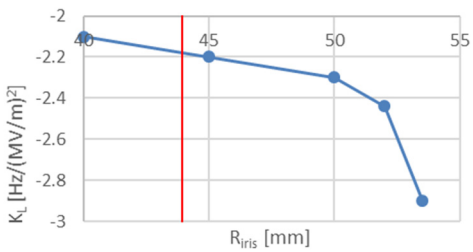

Figure 3: Trend of LFD versus R_{iris} (Based on a tentative cavity design with inner half-cell: D=203.0 mm, α= 7°, R=1, r=1.7, d= 14 mm and L =70.3 mm).

A similar study has also been done on the side-wall angle to understand its effect to LFD. Figure 4 shows the relationship between LFD and alpha. A smaller wall angle is favoured by LFD due to their monotonic dependence. In theory, a zero degree, vertical wall is the best choice for both the R/Q and LFD, but it may cause difficulties in the Field Flatness tuning stage and treatment procedures. To avoid a possible negative wall angle after tuning operation, a minimum acceptable value of 2° is chosen for our design.

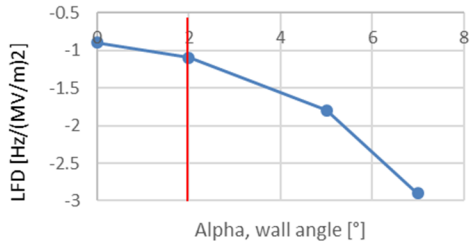

Figure 4: Trend of LFD versus wall angle (Based on a tentative cavity design with inner half-cell: R_{iris} =53.5 mm, D=203.0 mm , R=1, r=1.7, d= 14 mm and L =70.3 mm).

Other parameters, such as L, r, R and d are optimized based on their own functions. L is constrained by the geometric beta, namely 0.61. Iris elliptical ratio is adjusted to have a minimum E_{peak}/E_{acc}. Equator elliptical ratio R is set to 1 to obtain a round shape, beneficial to geometric factor G and to mitigate Multipacting. While a small d is favored by k_{cc}, but it may lead to difficulties for fabrication of the iris region. Hence, d is chosen according to the minimum requirement of fabrication.

EM Cavity Design

Based on the above consideration, the inner cell (IC) has been designed for LB650 cavity. Additional considerations are necessary in the design of the End Cell (EC). In fact, the EC contains the end tube for connecting the cavity into the string. The design of the EC must take into account these contributions to guarantee a proper resonance frequency and hence the required field flatness. Moreover, beam pipe diameter is required larger than iris aperture of inner cells to allow damping of HOM. A usual way to tune the EC, compensating for the extra volume of the beam pipe tube, is to create an extra volume in magnetic region near equator by tuning R (=B/A), but this may lead to a rectangular-like cell, critical for surface treatment and cleaning.

In our design, we use another strategy to tune the end cell by increasing the equator diameter, particularly effective when the beam pipe size is obviously larger than inner aperture, such as in our case. This approach can bring two advantages: almost round equator region, and the nearly symmetric end cell. As shown in Figure 5, a shape comparison of inner cell and end cell show good symmetry with respect to the cell centre. The equator radius of end cell indeed is 1.2 mm larger than the inner cell one.

ISBN: 978-3-95450-191-5 doi:10.18429/JACoW-SRF2017-TUPB070

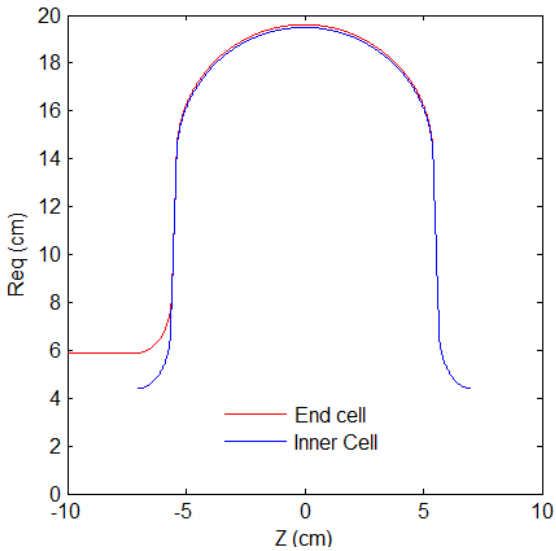

Figure 5: End-cell and inner-cell shapes of INFN-LASA design for PIP-II LB650 cavity.

Considering the compatibility with the interfaces of the cryomodule designed by Fermilab, including beam pipes, couplers, tuner and He tank, a design for PIP-II LB650 cavity is proposed by INFN-LASA, as shown in Table 2. Compared to FNAL design [6], we have increased obviously the cell-to-cell coupling with a slight sacrifice on R/Q and peak fields, but leading to a larger mode separation between π and 4/5 π modes.

Table 2: RF Parameters of INFN-LASA Design

Parameters	INFN-Design	FNAL_upd
β_{geo}	0.61	0.61
Frequency (MHz)	650	650
Number of cells	5	5
Iris diameter (mm)	88	83
Cell-to-cell coupling, k_{cc} (%)	0.95 (↗+23%)	0.75
Fre. sep. π-4π/5 (MHz)	0.57	
Eq. diameter – IC (mm)	389.8	389.9
Eq. diameter – EC (mm)	+2.3	
Wall angle – IC (°)	2	2
Wall angle - EC (°)	2	0.7
Effective length (10*L_{hc}, mm)	704	705
Optimum βopt	0.65	
Epeak/Eacc @βopt	2.40 (↗+3%)	2.33
Bpeak/Eacc (mT/(MV/m)) @βopt	4.48 (↗+2%)	4.41
R/Q (Ω) @βopt	340 (↘-4%)	356
G (Ω) @βopt	193	187

Figure 6 shows the fundamental modes in our design. Thanks to our special tuning procedure for end cells, we obtain a larger geometric factor G while keeping the side-wall angle always at 2°, avoiding potentially negative value during the cavity field flatness tuning stage.

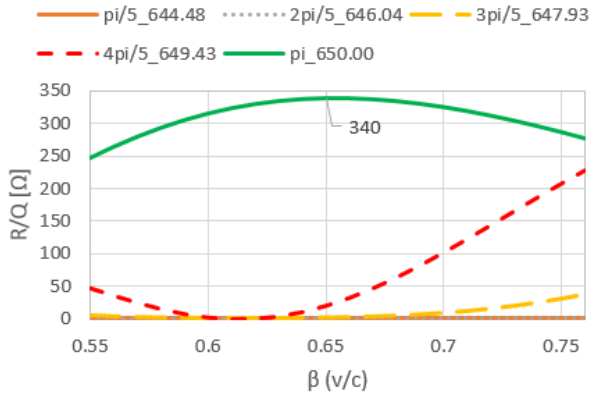

Figure 6: R/Q of fundamental modes in the beta range of LASA-design LB650 cavity (frequency in MHz).

High Order Mode Issue

We have assessed HOM risk in our cavity design, including cryogenic loss, longitudinal and transverse beam instabilities. Due to the relatively low beam current, we don't expect "Klystron-type" instability, and beam break up (BBU) instabilities induced by HOM [7, 8]. Concerning to the cryogenic loss that is mainly induced by HOM monopoles, attention needs to be paid to modes close to machine lines (ML), i.e. harmonics to 162.5 MHz, due to the possible frequency shift caused by fabrication tolerance.

The power loss induced by an exactly resonant HOM can be estimated by the formula: $P_{loss} \approx U_{HOM}^2/[(R/Q)Q_0]$, where $U_{HOM} = \frac{1}{2} I(R/Q)Q_L$, namely

$$P_{loss} \propto (R/Q)Q_L^2$$

Assuming maximum CW-operation current at $I = 5$ mA for PIP-II Linac, and $Q_0 = 10^{10}$ in the LB650 cavity, if we want P_{loss} much smaller than the sum of the static heat load and the cryogenic losses due to the accelerating mode, about 20 W per cavity [9], it requires the HOM: $(R/Q)Q_L^2 \ll 3 \times 10^{16}$.

In LASA-design LB650 cavity, the monopoles have been searched up to a band above cut-off frequency (f_{cut}) of beam pipe, at 1945 MHz. Among these, no trapped mode is found above f_{cut}, and below f_{cut}, there are only two pass-bands of HOM monopoles. In order to estimate the effect of these HOM if they are exactly shifted on the ML, we simulate their max R/Q in the accelerating beta range and their loaded Q with the antenna geometry provided by FNAL [6]. In simulation, we assume a coaxial-line-like coupler, and fully matched termination at the coupler end.

Figure 7 shows all the $(R/Q)Q_L^2$ for the HOM monopoles under f_{cut}. As we can see, all of them are much smaller than 3×10^{16}, hence their HOM-induced power loss will be negligible. Among these modes, two of them are trapped-like, one at 1470.5 MHz and the other at 1618.5

ISBN: 978-3-95450-191-5 doi:10.18429/JACoW-SRF2017-TUPB070

MHz, being last mode in each passband, respectively, as shown in Figure 8. The later one has the maximum potential power loss in these two passbands.

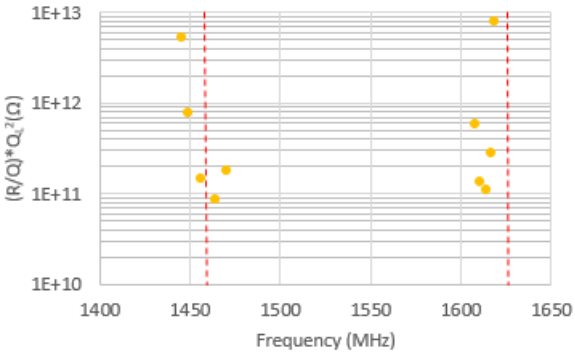

Figure 7: HOM monopoles under cut-off frequency in INFN-LASA LB650 cavity (red lines denote machine lines).

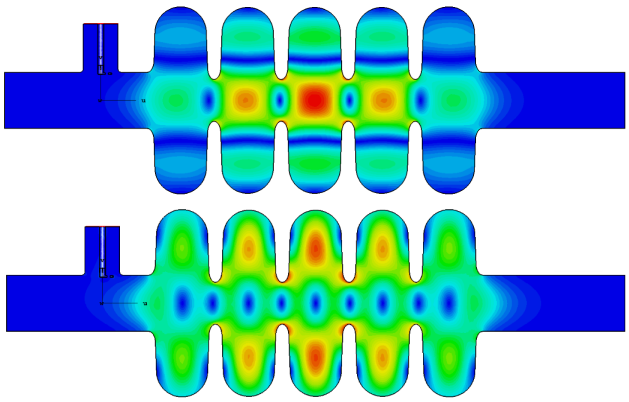

Figure 8: (Upper) Last mode in 2nd monopole passband, +8 MHz away from 9th ML, with maximum R/Q=0.1 Ω and Q_L=1.4 × 10^6; (lower) last mode in 3rd monopole passband, -6.5 MHz away from 10th ML, with with maximum R/Q = 24.0 Ω and Q_L=5.7 × 10^5.

It is worth to mention that in the simulation, we used the default distance of antenna tip to axis at 54 mm, corresponding $Q_{ext} = 1.3 \times 10^7$ for the accelerating mode, 20% higher than the required value. It means that with the required Q_{ext} for π-mode, the loaded Q for HOM will be even lower. Besides, due to the R/Q dependence on beta, an average value will be less than the maximum R/Q used in the calculation. Both these two points will further decrease the HOM induced power loss.

Concerning the above preliminary study, we do not expect danger from HOM effect in our cavity. Nevertheless, studies on full HOM modes finding and the more detailed HOM frequency shift due to fabrication tolerance are undergoing.

Regarding Multipacting, we do not foresee any limitation to the cavity performance based on our round-like-equator cells. Due to its ubiquity in superconducting cavity, the studies on Multipacting will also be carried out.

Mechanical Design

Due to the narrow bandwidth of the accelerating mode, mechanical design is especially important for controlling both Lorentz force and microphonic detuning. With the capacity to be operated in CW mode, the microphonic one is even more critical in the design.

Considering standard Niobium mechanical parameters, a cavity thickness at 4.2 mm is chosen based on our study, balancing between the cavity stiffness and heat conducting. We apply stiffening rings both at end cell and at inner cells to provide enough suppression of detuning. Comparing to double stiffening rings between inner cells, one stiffening ring is preferred due to its sufficiency and simplicity. Figure 9 is the 3D drawing of the cavity with the single stiffening rings.

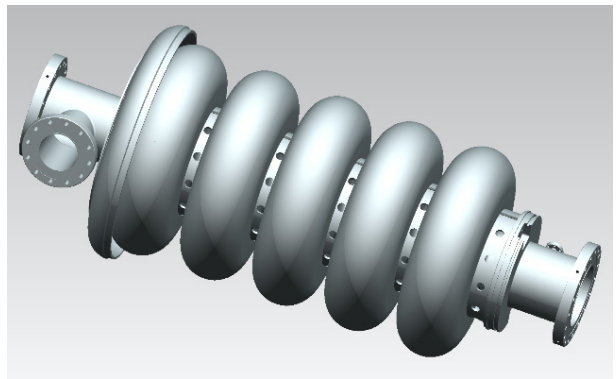

Figure 9: 3D rendering of the cavity with single stiffening ring on all irises.

LFD coefficient and pressure sensitivity of this design are shown in Figure 10 and Fig. 11, respectively. Our study shows a best LFD suppression with inner stiffening rings at radius of about 70 mm, while microphonic suppression prefers larger radius.

The latter is even more important in CW operation; hence it is emphasized in our case. After balancing LFD and microphonics contributions, a radius of 100 mm for both inner and external (outer irises) stiffening rings is chosen.

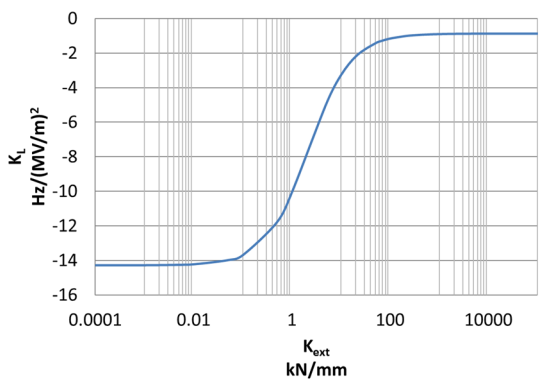

Figure 10: Lorentz Force Detuning coefficient vs External Stiffness.

ISBN: 978-3-95450-191-5 doi:10.18429/JACoW-SRF2017-TUPB070

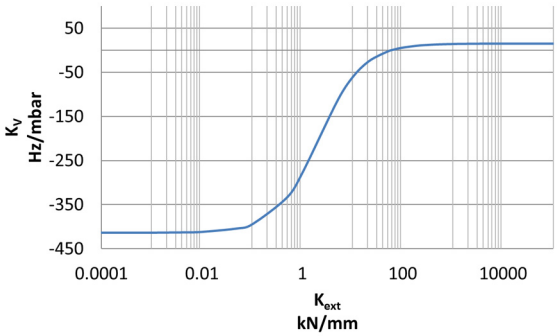

Figure 11: Pressure sensitivity vs external stiffness.

Figure 12 shows the stress pattern on the cavity profile in case of a pressure test.

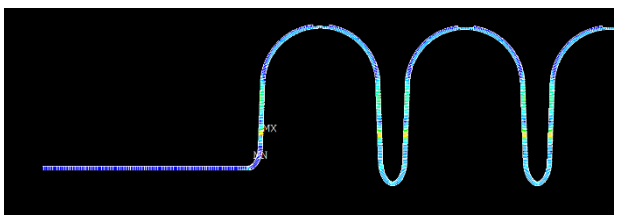

Figure 12: Stress profile under internal pressure.

The mechanical design parameters, based on the previous discussed considerations, are summarized in Table 3.

Table 3: Mechanical Parameters of LB650 Cavity of INFN-LASA Design

Parameter	INFN-LASA design
Inner stiffening Radius	100 mm
External stiffening radius	100 mm
Stiffness	2.17 kN/mm
Frequency sensitivity	213 kHz/mm
LFD @ 68 kN/mm	-1.28 Hz/(MV)^2
Pressure sensitivity @ 68 kN/mm	2.0 Hz/mbar
Maximum Pressure @ 50 MPa	3.9 bar
Maximum Displacement @50 MPa	1.8 mm

The search for the right compromise led us to a final solution that reduces the pressure sensitivity close to zero, only with a negligible loss on the LFD response, compared to the FNAL specs (-1.2 Hz/(MV)^2).

PRODUCTION

In order to validate our cavity design and the procedures of fabrication and surface treatments, we are producing 3 single-cell cavities, two in large grain Nb and the other in fine grain. The 3D drawing is shown in Fig. 13.

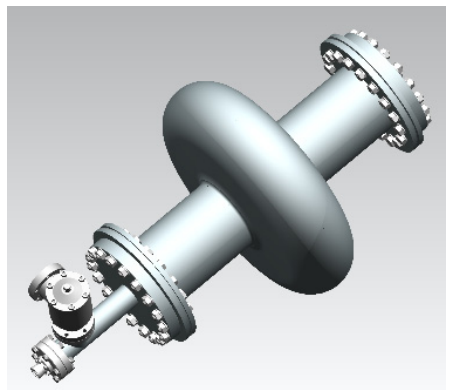

Figure 13: 3D drawing of single-cell cavity.

The single cell cavities are planned to be fabricated in industry, EP surface treated, and finally vertical tested in INFN-LASA within the existing cryostat. Nevertheless, several upgrading of infrastructure has to be done, including supporting frame on insert.

CONCLUSION

INFN-LASA, a potential international partner to Fermilab PIP-II project, has proposed a new design of LB650 cavity. We have studied the criteria for cell-to-cell coupling, the effect of Lorentz Force Detuning and microphonic versus cavity geometric parameters. Based on the minimum acceptable cell-to-cell coupling, we have designed a cavity with highest accelerating efficiency, and with good suppressing of LFD and microphonic detuning by choosing the proper radius of single stiffening rings. In particular, the cavity is designed with slightly larger end cells to provide both good field flatness and quasi-symmetric geometry with almost round equator. Preliminary study on HOM shows no danger to both the beam stability and cryogenic loss. Three single-cell prototype are being started to verify the design and relative procedure.

REFERENCES

[1] A. Saini *et al.*, "Design of Superconducting CW Linac for PIPII", in *Proc. IPAC'15*, Richmond, VA, USA 2015.

[2] J. Sekutowicz *et al.*, "Low Loss Cavity for the 12 GeV CEBAF Upgrade", JLAB, TN-02-023, June (2002).

[3] D. Nagle *et al.*, "Coupled resonator model for standing wave accelerator tanks", *RScI*, vol. 38, 1583-1587.

[4] J.F. Chen *et al.*, "Improvement of Buildcavity code", in *Proc. SRF'15*, Whistler, BC, Canada, 2015.

[5] SUPERFISH, http://laacg.lanl.gov/laacg/services/serv_codes.phtml

[6] T. Khabiboulline, "LB650 cavity RF design update", Internal technical report, March 29, 2016.

ISBN: 978-3-95450-191-5 doi:10.18429/JACoW-SRF2017-TUPB070

[7] S.H. Kim, "HOM Experiences at the SNS SCL", SPL HOM Workshop at CERN, June 25-26, 2009.

[8] S. A *et al.*, "Higher-order-mode analysis of the PEFP low-beta superconducting RF linac", *Journal of the Korean Physical Society ,vol*. 50, 1421-1426 (2007).

[9] M. Bal *et al*., "The PIP-II conceptual design report", October 10, 2016.